Proceedings of Meetings on Acoustics

OCTOBER 10 2024

Lauren Krebs; Whitney Coyle; Eric Rokni; Ashley Cannaday

54, 035005 (2024)
https://doi.org/10.1121/2.0001940

Proceedings of Meetings on Acoustics
Volume 54 http://acousticalsociety.org/

13-17 May 2024

Musical Acoustics: Paper 2aMU7

ULJKLRRWWJ LWRSLS

Lauren Krebs Schefter, Whitney Coyle, Eric Rokni and Ashley C
Department of Physics, Rollins College, Winter Park, FL, 32789; lschefter@rollins.edu 9
wcoyle@rollins.edu; erokni@rollins.edu; ashley@rollins.edu

Amppcarjw npcbgargle rfc nj_wgle dpcosclagcq md
pcqml_rmp ugrf rfc _bbgrgml md _l clb amppcargml
ncpf_nq rfc qgknjcqr `cgle rf_r rfc clb amppcarg
npcqqspc qr_lbgle u_tc glqgbc rfc ngnc, Fmuctcp*
dmslb _l slcvncarcb cvnmlclrg_j bca_w md npcqqspc
rfmqc dglbgleq _amsqrga_jjw, ? djsc mpe_l ngnc u_
hsqr glqgbc _lb gkkcbg_rcjw msrqgbc rfc clb md rf
Kgapmdjmul qmslb glrclqgrw npm`c, Rfcqc kc_qspckc
_lb amkn_pcb rm rfc mnrga_j gk_ecq, Ufgjc _l cvn
emmblcqq+md+dgr _nnc_pq rm `c bcnclbclr ml ufgaf
md _ nmrclrg_j rp_lqgrgml_j pcegml* _qqcqqgle rfc
_lb qgxc'* _lb gltcqrge_rgle nmrclrg_j qclqmp glr

Published by the Acoustical Society of America

1. INTRODUCTION

The flue organ pipe has a very simple geometry, which can be seen in Fig. 1, and is an ideal instrument to begin studying various acoustical phenomena. After a somewhat complicated generator (the fipple area), the flue organ pipe has no tones holes and consists of a long, straight pipe. The instrument does not have a reed, which means it can be simply modeled as an open-open pipe resulting in a spectrum that includes all harmonics.

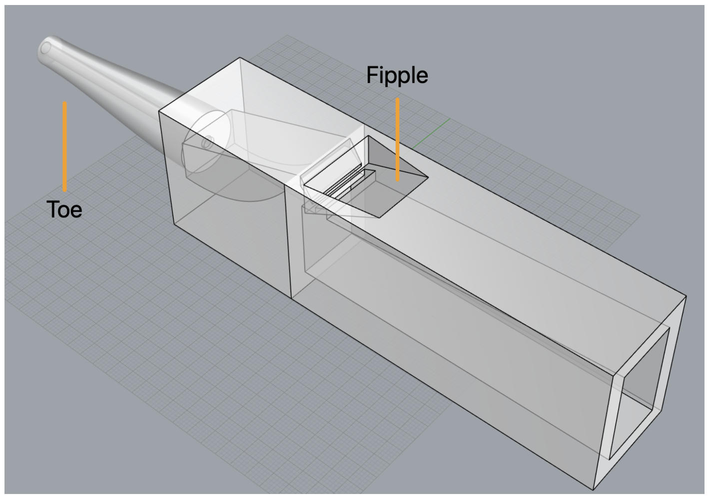

Figure 1: 3D rendering of the organ pipe used in this work. The toe (or location of air input) is located on the upper left, and the fipple can be seen in the center. Varying lengths of resonators can be attached to the far end of the pipe (bottom right).

When air flows through the toe of organ pipe (the far left end in Fig. 1), the pressure difference across the mouth (just before the fipple) causes the air to oscillate in and out of the mouth which eventually creates a standing wave inside the resonator or body of the pipe. At the far end of the pipe, where the sound is radiated, there is an "end-correction" and the acoustical length of the standing wave is not the same as the physical length of the pipe when modeled.[1] In other words, the final node of the standing wave is not considered to be at the end of the pipe, but slightly after the physical end. The end correction theory states that the standing wave and its properties also continue beyond the physical end of the pipe, as shown in Fig. 2. The equation,

$$\delta = a(0.6133 - 0.1168[ka]^2), \tag{1}$$

was experimentally derived by Levine and Schwinger and shows that length of this "end-correction" (δ) region can be calculated using the radius of the pipe (a) and the wave number (k), which is directly proportional to the measured frequency.

2. BACKGROUND

In 2023, Moore et al. published a JASA Express letter describing optical studies of the standing wave behavior near the the end of the flue organ pipe.[2] The group used an optical setup known as transmission electronic speckle pattern interferometer (TESPI) to image the flow inside and just

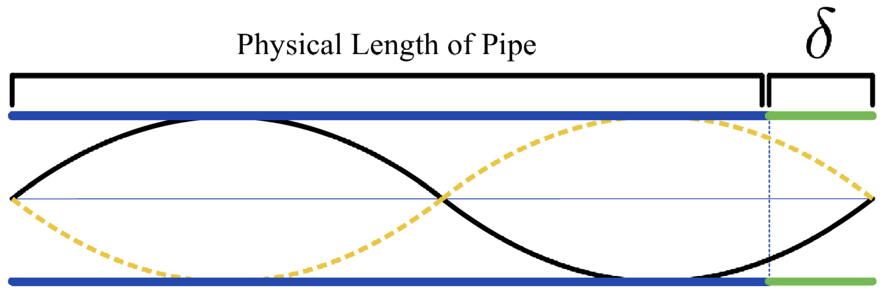

Figure 2: The end correction theory states the standing waves continues beyond the physical length of the pipe (blue). The distance of the region, δ (green), can be calculated using Eq 1.

outside a flue organ pipe. By filtering the fundamental frequency, the standing wave inside the pipe and in the end correction region was visualized. Unexpectedly, Moore et al. found an internal node in the pressure just before the end of the pipe, followed by an exponential decay in pressure in the end correction region, shown in Fig. 3. From the end correction theory, they expected a sinusoidal decay to the final node, just like any other node inside the pipe. These results inspired our current work using acoustical sensors to investigate the same region.

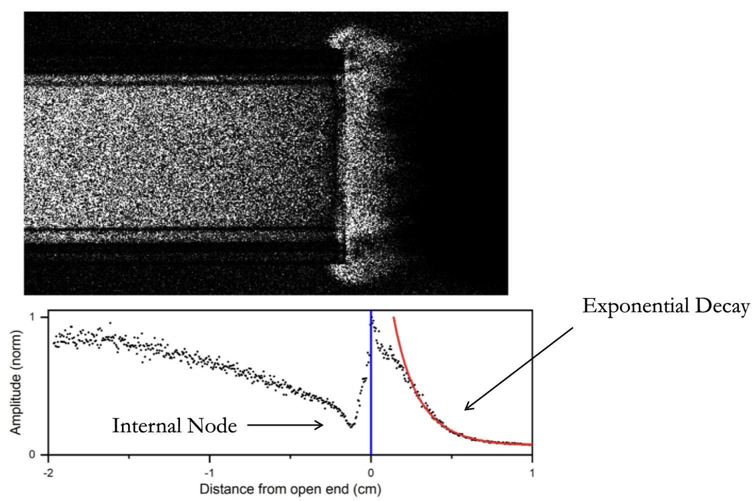

Figure 3: Moore et al.'s results from their optical work. The top figure shows the image acquired using TESPI and the bottom image shows the amplitude of the pressure first inside then outside of the organ pipe. Notice the exponential decay outside of the pipe. [Modified from Moore[2]]

Other groups have explored the behavior at the end of the pipe both computationally and experimentally. For instance, in 2017 Kirby and Duan investigated the end of a pipe using a computational model.[3] While they did find an internal node in one case, their simulations were at high flow rates which do not necessarily correlate with the observations in musical instruments. On the other hand, in 2014 Rucz et al. experimentally investigated the end of the organ pipe with a microphone and did not note any unexpected behavior.[4] However, it is not clear how similar their measurement techniques are compared to Moore et al. To our knowledge, there has been no study similar enough to the optical investigations. The goal for this work was to use the same experimental setup as Moore et al. to perform acoustical measurements, instead of their optical measurements, that would allow for a more direct comparison.

3. METHODS

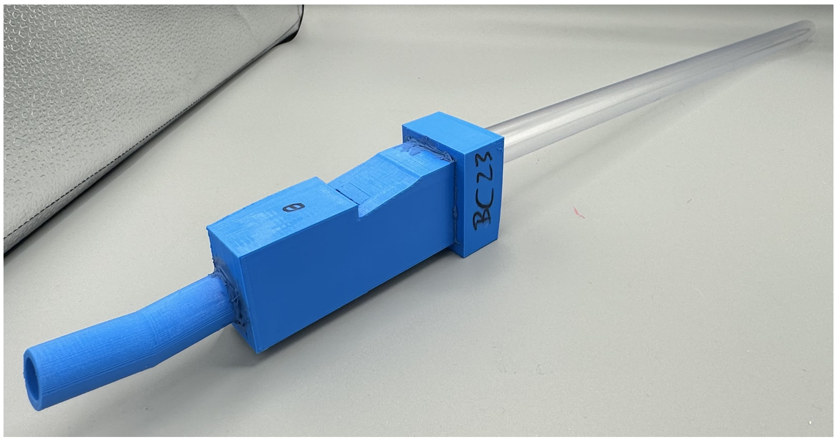

Figure 4: The organ pipe (generator) in blue was printed from PLA using the Makerbot Replicator+. The tube (resonator) was made from plexiglass and was attached to the generator ($L =$ 48 cm, $r =$ 1 cm).

A flue organ pipe was modeled and 3D printed using resources in our lab (Rhino7 and Makerbot Replicator+), shown in Fig. 4. Then, a plexiglass tube that was 48 cm in length and 1 cm in radius was attached to the organ pipe body. 3D printing the body of the organ pipe allows customization to fit best in the setup and have a working design where the geometry can vary for future experiments.

The flue organ pipe was driven at three different harmonics with a compressed air source. For this length of tubing the measured first harmonic was 288 Hz, the measured fifth harmonic 1460 Hz, and the measured seventh harmonic 2075 Hz. A flowmeter (GR series by Fathoms Technology) was used between the compressed air and the organ pipe to ensure the blowing pressure of the driven airflow was consistent across trials.

Measurements of the end of the pipe were made using a zero-degree sound intensity probe by MicroFlown. This MicroFlown sensor is 0.59 cm in length and 0.4 cm in radius. The sensor acquires pressure measurements and particle velocity measurements. For the work described in this paper, only the pressure measurements are shown and discussed. The MicroFlown was mounted on a horizontal translation stage to make sure the increments were as precise as possible. Starting 0.254 cm inside from the end of the pipe, the MicroFlown was translated about 2.29 cm, ending 2.032 cm outside of the pipe. Every 0.0254 cm, a pressure measurement was taken, allowing for 70 measurements from every trial. The measured region included just inside the pipe, physical end of the pipe, the end correction, and beyond. The experimental setup is depicted in Fig. 5. This process was repeated three times for each of the three harmonics. However, as there was nothing unique about the fifth harmonic data compared to the first harmonic data only the low and high frequencies were analyzed.

As the MicroFlown sensor measured the oscillations in the pipe, it was recording the uncalibrated pressure values over time. These measurements were not converted to pascals because only

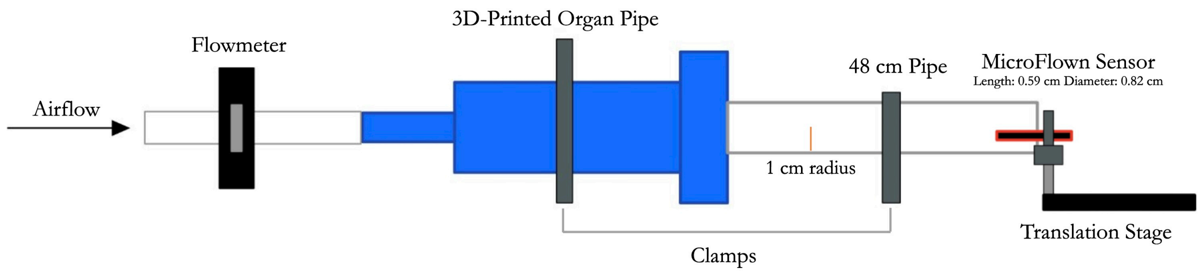

Figure 5: Experimental apparatus with the 3D printed organ pipe driven by a compressed air source (from the left). Measurements of the end of the pipe were made using a sensor on a horizontal translation stage.

the relative shape of the curves were of importance. The duration of each individual measurement was 23 milliseconds and the sampling rate was 44.1 khz. The data were analyzed in MATLAB. The analysis code calculated the root mean squared (RMS) values for every data point and plotted them versus the distance travelled horizontally in the tube. In Fig. 6 and Fig. 7 each measurement of pressure oscillating over time is represented with a data point as an RMS pressure value with arbitrary units at a distance from the end of the pipe in mm. These data were then input to MATLAB's curve-fitting toolbox that creates comparison plots, where custom equations can be added to fit the data and exclude regions of data from the fitting parameters.

4. RESULTS AND ANALYSIS

From the end correction theory, the standing wave created inside the driven organ pipe is assumed to be sinusoidal up until the acoustical end, (δ) away from the physical end of the pipe. Beyond the acoustical end of the pipe, the wave can be expected to decay as $1/R$ since the then travelling wave sound will decay spherically. When the pressure was expected to decay sinusoidally inside the end correction, the data was fit to a sinusoid,

$$y = A\sin(kx + \phi) + z, \tag{2}$$

where A, z, and ϕ are the curve-fitting parameters and k is the wave number that was calculated from the measured frequency. The pressure inside of the pipe was measured when driven at the low and high harmonic. The low harmonic data are plotted in Fig. 6a and the high harmonic data are plotted in Fig. 7a. When the pressure was expected to decay as $1/R$ beyond the end correction, the data was fit to the rational function,

$$y = \frac{A}{x + \delta} + z, \tag{3}$$

where A and z are the fitting parameters and δ is the value calculated using Eqn. 1. The pressure in this region beyond the end correction was measured while the organ pipe was driven at the low and high harmonic. These measurements were analyzed in MATLAB and the low harmonic data are plotted in Fig. 6b and the high harmonic data are plotted in Fig. 7b.

From preliminary visual observation, both of these curves seem to be valid fits for the data points in the respective regions. To quantify the goodness of fit, MATLAB calculates the sum of

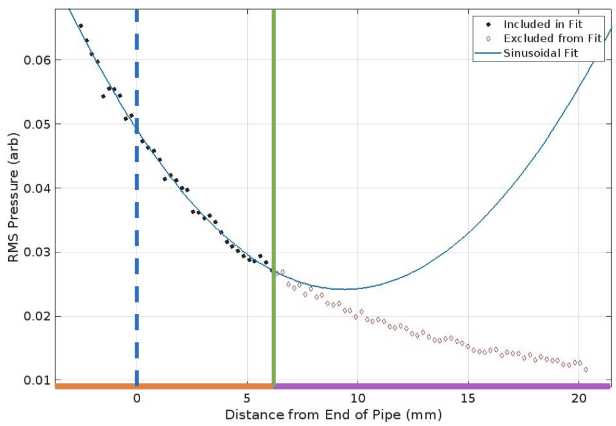

(a) Inside end correction where a standing wave is assumed and a sinusoidal decay in pressure is expected, therefore the data is fit to Eqn. 2.

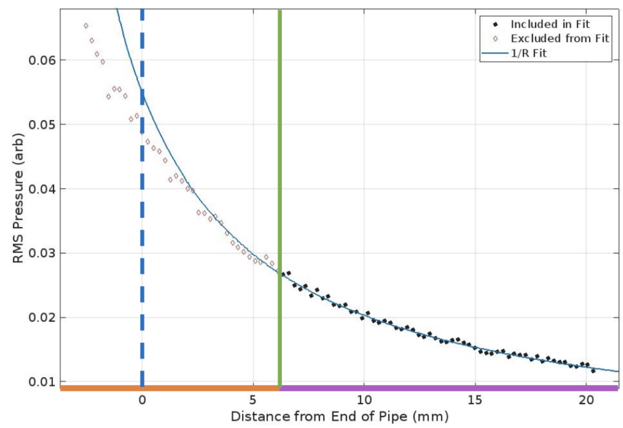

(b) Outside end correction where a travelling wave is assumed and a $1/R$ decay in pressure is expected, therefore the data is fit to Eqn. 3.

Figure 6: Low harmonic data: dashed blue line is physical end of the pipe at zero, green line is the calculated end correction (δ= 0.6099 cm) value from Eqn. 1, the orange region indicates where a standing is assumed, and the purple region indicates where the travelling wave is assumed.

squared errors (SSE). A value close to 0 indicates that the fitting equation has a smaller random error component, leading to a more useful prediction of behavior when using the fit. For the data in Fig. 6a and Fig. 6b, the SSE values were both less than 0.0001, verifying the observations and matching the expectations that the pressure is decaying sinusoidally inside the end correction and as $1/R$ beyond the end correction.

Eqn. 2 fits the data in Fig. 7a well merely from visual observation. The SSE value for the fit within the end correction region at the high harmonic is 0.0002, confirming the goodness of fit. However, beyond the end correction, it is clear that Eqn. 3 is not a valid fit for the pressure decay in this region and the SSE value confirms that equating to 0.025. Compared to the three other fits, this SSE value is less close to zero.

5. DISCUSSION AND CONCLUSION

Aside from the two straightforward fits shown in the previous sections and either including the data completely inside or outside the pipe, we are trying an array of other fit compositions. One such fit is $\sin(kx + \phi) + 1/R$ to represent the contribution from both the standing wave and the traveling wave outside of the pipe. Not shown in this paper, the SSE value was sufficiently low, however it is still better when applied to the low harmonic than to the high harmonic. Nevertheless, in this preliminary stage, this mixed fit seemed to be an improvement from strictly the $1/R$ fit.

Overall, in this work, we explored the acoustical behavior at the end of the organ pipe using a MicroFlown sensor. As expected, the pressure values oscillated sinusoidally inside the end correction region. After the end correction, we expected to see a clear $1/R$ decay in pressure but this was only true for the low frequencies. The high frequencies on the other hand, had inconsistencies, as was also noted by Moore et al. for which we do not yet have an explanation. It is possible that the

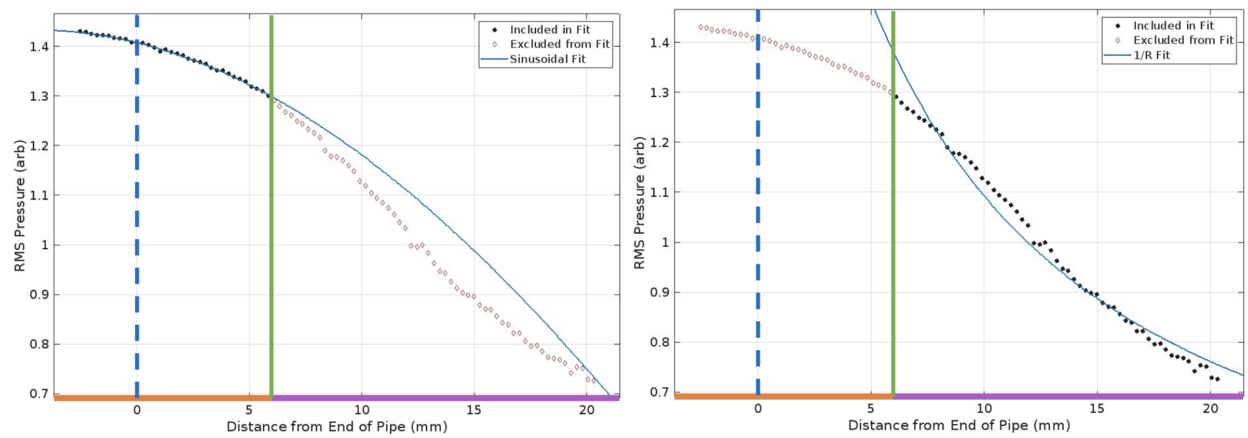

(a) Inside end correction region where a standing wave is assumed and a sinusoidal decay in pressure is expected, therefore Eqn. 2 was fit to the data.

(b) Outside end correction where a travelling wave is assumed and a $1/R$ decay in pressure is expected, therefore Eqn. 3 was fit to the data.

Figure 7: High harmonic data: dashed blue line is physical end of the pipe at zero, green line is the calculated end correction (δ= 0.5936 cm) value from Eqn. 1. Orange region indicates where a standing is assumed, and purple region indicates where the traveling wave is assumed.

relatively poor agreement observed in Fig. 7b may be attributed to the sound radiation characteristics at the pipe's end. Specifically, as frequency increases, the sound radiation exhibits a more extended nearfield, causing the transition to the 1/R farfield behavior to occur more gradually at higher harmonics

In the future we plan to continue experimentally exploring different combinations of curve fitting equations, such as the $\sin(kx + \phi) + 1/R$, with the data we already measured. We also plan to use the Microflown sensor to take measurements around the inside and outside edges of the tube (as opposed to down the central axis) to better understand the behavior of the flow see whether this sheds any more insight into the behavior that Moore at al. observed (such as the internal node).[2]

Computationally, we plan to compare our experimental results with various simulation models such as the Lattice Boltzmann Method (LBM) as well as COMSOL models. The issue with the computational models, for the time being, is that we will only be able to compare the low frequency behavior due to the computational time/resources required. Nevertheless, computational explorations will be useful (and necessary) to further understanding the behavior of the supposedly simple musical instruments.

6. ACKNOWLEDGEMENTS

The authors wish to thank T. Moore, M. Griffin, and N. Giordano for their contributions to this work. The authors gratefully acknowledge funding from the National Science Foundation Award #2109932 and the Rollins College Student Faculty Collaborative Scholarship Program.

REFERENCES

[1] H. Levine and J. Schwinger, "On the Radiation of Sound from an Unflanged Circular Pipe," Physical Review, vol. 73, no. 4, pp. 383–406, Feb. 1948, doi: https://doi.org/10.1103/physrev.73.383.

[2] T. R. Moore, M. S. Kellison, and W. L. Coyle, "The behavior of standing waves near the end of an open pipe with low mean flow," JASA express letters, vol. 3, no. 5, May 2023, doi: https://doi.org/10.1121/10.0019500.

[3] R. Kirby and W. Duan, "Elastic wave propagation in liquid filled buried pipes," Paper presented at 24th International Congress on Sound and Vibration, ICSV 2017, London, United Kingdom. Jan. 2017.

[4] P. Rucz, F. Augusztinovicz, J. Angster, T. Preukschat, and A. Miklós, "Acoustic behavior of tuning slots of labial organ pipes," The Journal of the Acoustical Society of America, vol. 135, no. 5, pp. 3056–3065, May 2014, doi: https://doi.org/10.1121/1.4869679.